DOI: 10.1002/anie.201004537

Microporous Materials

Metal–Organic Frameworks with Incorporated Carbon Nanotubes: Improving Carbon Dioxide and Methane Storage Capacities by Lithium Doping**

Zhonghua Xiang, Zan Hu, Dapeng Cao, Wantai Yang,* Jianmin Lu, Bingyong Han, and Wenchuan Wang*

Reduction of the anthropogenic emission of CO_2 is currently a top priority because CO_2 emission is closely associated with climate change. Carbon capture and storage (CCS)[1] and the development of renewable and clean energy sources are two approaches for the reduction of CO_2 emission. One of the most promising alternative fuels is CH_4, which is the major component of natural gas. The efficient storage of CH_4 is still one of the main challenges for its widespread application. Accordingly, the development of more efficient approaches for CO_2 capture and CH_4 storage is critically important.

Recently, metal–organic frameworks (MOFs, e.g., MOF-210 and NU-100)[2] have shown great potential for gas storage because of their high specific surface area (SSA) and functionalized pore walls. However, most MOF materials still show relatively low CO_2 and CH_4 uptakes. To enhance CO_2 and CH_4 adsorption, it is imperative to develop new materials, such as covalent organic frameworks (COFs),[3] or to modify MOFs by using postsynthetic approaches.[2b,4] Herein, we focus on the latter strategy. One of the modification approaches is incorporation of carbon nanotubes (CNTs) into MOFs in order to achieve enhanced composite performance, because of the unusual mechanical and hydrophobicity properties of CNTs.[5] Another approach is doping MOFs or COFs with electropositive metals.

Recent studies indicate that the surface carboxylate functional groups of a substrate could act as nucleation sites to form MOFs by heterogeneous nucleation and crystal growth.[6] Both experimental and theoretical investigations indicate that the H_2 adsorption capacities of MOFs can be enhanced significantly by doping alkali-metal ions, in particular Li^+ ions, to the frameworks, owing to the strong affinity of Li^+ ions towards H_2 molecules.[3d,7] Similarly, Lan et al. also showed theoretically that doping of COFs with Li^+ ions can significantly enhance the CH_4 uptake of COFs.[8] Most recently, the multiscale simulations performed by Lan et al. indicate that Li is the best surface modifier of COFs for CO_2 capture among a series of metals (Li, Na, K, Be, Mg Ca, Sc and Ti).[9] Furthermore, their simulations show that the excess CO_2 uptakes of the lithium-doped COFs can be enhanced by four to eight times compared to the undoped COFs at 298 K and 1 bar.[9]

Motivated by these experimental and theoretical results, we synthesized hybrid MOF materials by using the two modification techniques outlined above, that is, 1) incorporation of CNTs into $[Cu_3(C_9H_3O_6)_2(H_2O)_3]\cdot x\,H_2O$ ($[Cu_3(btc)_2]$, HKUST-1; btc = 1,3,5-benzenetricarboxylate), which is an important MOF material owing to its open metal sides and high thermal stabilities, as well as its sorption properties,[2a,10] and 2) doping $[Cu_3(btc)_2]$ with Li^+ ions. We used lithium naphthalenide ($Li^+C_{10}H_8^-$) to introduce Li^+ ions into the $[Cu_3(btc)_2]$ frameworks. These frameworks have Cu^{2+} sites that become available for interaction with other molecules after removal of H_2O in from Cu^{2+} carbonyl complexes, and can also be easily rehydrated without change of the crystalline nature of the material after exposure to air[11] (see Figure S1 in the Supporting Information). Although the btc ligand can not act as an electron receptor for the electron transfer from the naphthalenide radical anion,[7c] the rehydration of the Cu^{2+} sites in the framework makes the electron transfer possible because of the strong nucleophilicity of lithium naphthalenide, which is the main reason for selecting this complex. Furthermore, we also proposed a hypothetical hybrid composite, in which the CNTs with carboxylic groups provide homogeneous nucleation sites to support a continuous copper framework growth, and the Li^+ ions were subsequently introduced into the frameworks. To better explore the cooperative effects of CNT incorporation and Li doping on the uptakes of CO_2 and CH_4, we have prepared four different MOF materials. The first two MOFs are unmodified $[Cu_3(btc)_2]$ MOF (**1**); lithium-doped $[Cu_3(btc)_2]$ ($Li@[Cu_3(btc)_2]$). The sample of $Li@[Cu_3(btc)_2]$ with Li/Cu = 0.07 is denoted as **1**·Li, which exhibits the greatest gas uptake of the investigated samples with various Li contents. We also prepared a carboxylic CNT hybrid composite

[*] Z. Xiang, Z. Hu, Prof. Dr. D. Cao, Prof. W. Wang
Division of Molecular and Materials Simulation
Key Lab for Nanomaterials, Ministry of Education
Beijing University of Chemical Technology
Beijing 100029 (China)
Fax: (+86) 10-6442-7616
E-mail: caodp@mail.buct.edu.cn
Homepage: http://www.ms.buct.edu.cn
Prof. W. Yang, Dr. J. Lu, Prof. B. Han
College of Materials Science and Engineering
Beijing University of Chemical Technology
Beijing 100029 (China)
E-mail: yangw@mail.buct.edu.cn

[**] This work was supported by the Huo Yingdong Foundation (121070), the National 973 Program (2011CB706900, 2007CB209706), National Scientific Research Funding (ZD0901), the NSF of China (20736002), and the Chemical Grid Program from BUCT.

Supporting information for this article is available on the WWW under http://dx.doi.org/10.1002/anie.201004537.

(CNT@$[Cu_3(btc)_2]$, **2**) and lithium-doped CNT@ $[Cu_3(btc)_2]$ (Li@CNT@$[Cu_3(btc)_2]$; the sample with Li/Cu = 0.001 is denoted as **2**·Li.)

Unmodified $[Cu_3(btc)_2]$ was synthesized by following our previously reported procedure.[10b] To obtain homogeneous nucleation sites, we treated multiwalled CNTs (MWCNTs) with a mixture of nitric acid and sulfuric acid (1:1 v/v) to introduce carboxylic groups into the CNT surface, which is confirmed by IR and X-ray photoelectron spectroscopy (XPS; Figures S2 and S3 in the Supporting Information). MOF **2** was synthesized by reaction of carboxylic multiwalled CNTs (0.2 mg), $Cu(NO_3)_2{\cdot}3H_2O$ (5 g), and btc (2.5 g) in a mixture of DMF/water/ethanol 1:1:1 at 85 °C. The frameworks were immersed in a solution of lithium naphthalenide in tetrahydrofuran (THF). The powder X-ray diffraction patterns (PXRD; Figure S4 in the Supporting Information) of **1**, **1**·Li, **2**, and **2**·Li are consistent with the simulated patterns,[10a] thus indicating that incorporation of CNTs and the introduction of Li^+ ions do not disrupt or destroy the crystal structure of $[Cu_3(btc)_2]$. Thermogravimetric (TG) analysis (Figure S5 in the Supporting Information) shows that all four compounds possess high thermal stability, and the deformation of these framework structures occurs after 300 °C (Figure S5 in the Supporting Information). Weight loss is hardly observed in the range $200 < T < 300$ °C for **1**·Li, **2**, and **2**·Li, while the TG trace of **1** gradually decreases before 300 °C, thus indicating that the guest solvent is released more effectively from **1**·Li, **2**, and **2**·Li than from **1**.

The PXRD patterns of **2** (Figure S4 in the Supporting Information) show a high-intensity $[Cu_3(btc)_2]$ peak that masks the characteristic CNT (002) peak, which normally appears at $2\theta = 26$–$27°$. However, transmission electron microscopy (TEM) reveals that the CNTs are indeed well admixed with $[Cu_3(btc)_2]$. The CNTs, which act as composite fillers in the microcrystal, can be seen from the TEM image at low magnification (Figure 1a). High-resolution hybrid composite lattice images (Figure 1b,c) also show two distinctive lattice spacings of 0.203 and 0.33 nm, which correspond to the interlayer spacing values for the (1082) plane of $[Cu_3(btc)_2]$ and the (002) plane of the multiwalled CNTs, respectively. These results therefore indicate that the CNTs are incorporated in $[Cu_3(btc)_2]$. It is assumed that the $[Cu_3(btc)_2]$ crystals are formed by heteronucleation and crystal growth on the carboxylic groups of the CNT.[4a] However, it is very difficult to characterize the interface region of CNTs in the frameworks by using available techniques. The profile of the N_2 adsorption isotherm of **2** is similar to that of **1** (Figure S6 in the Supporting Information). As shown in Table 1, the BET SSA of **2** (1458 $m^2 g^{-1}$) is close to that of **1** (1587 $m^2 g^{-1}$). However, the pore volume of **2** (0.87 $cm^3 g^{-1}$) is larger than that of **1** (0.73 $cm^3 g^{-1}$). This result further suggests that the crystal growth on the MWCNTs with carboxylic groups subsequently provides a route for removal of guest solvent molecules during activation and leads to a larger pore volume.[4a]

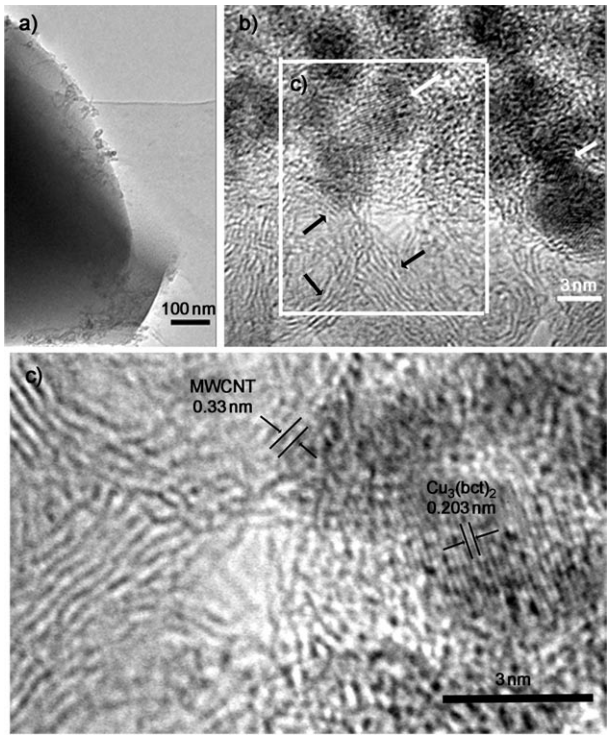

Figure 1. TEM images at a) low magnification and b) high magnification (white and black arrows represent lattice images of $[Cu_3(btc)_2]$ and multiwalled CNTs, respectively). c) Expansion of the boxed area in (b).

To determine how modification by CNTs affected the CO_2 and CH_4 capacities of $[Cu_3(btc)_2]$, we carried out the gas adsorption measurements by using an intelligent gravimetric analyzer (IGA-003). Both CO_2 and CH_4 isotherms for **1** and **2** show good reversibility without hysteresis and are not saturated (Figure 2). At 298 K and 18 bar, the CO_2 uptake of **2** is 595 mg g^{-1}, which is about twice the uptake of **1** (295 mg g^{-1}) under the same conditions (Table 1). Similarly, the same behavior occurs for the CH_4 adsorption. At 298 K and 18 bar, the capacity of **2** for CH_4 reaches 120 mg g^{-1}, which is higher than the value for **1** (72 mg g^{-1}). Thus, the

Table 1: Summary of adsorption properties of **1**, **1**·Li, **2** and **2**·Li.

Materials	Li/Cu [mol mol^{-1}]	BET SSA[a] [$m^2 g^{-1}$]	Pore volume[b] [$cm^3 g^{-1}$]	CO_2 uptake[c] [mg g^{-1}]	CO_2 uptake per effective SSA[c] [mg m^{-2}]	Q_{st}[d] [KJ mol^{-1}]	CH_4 uptake[c] [mg g^{-1}]	CH_4 uptake per effective SSA[c] [mg m^{-2}]
1 (unmodified $[Cu_3(btc)_2]$)	0	1587	0.73	295	0.19	28.0	72	0.05
1·Li (Li@$[Cu_3(btc)_2]$)	0.07	795	0.51	469	0.59	35.7	96	0.12
2 (CNT@$[Cu_3(btc)_2]$)	0	1458	0.87	595	0.41	34.0	120	0.08
2·Li (Li@CNT@$[Cu_3(btc)_2]$)	0.001	857	0.69	660	0.77	36.8	130	0.15

[a] BET SSA calculated in the region $P/P_o = 0.05$–0.3. [b] Determined at $P/P_o = 0.9997$. [c] Uptake at 298 K and 18 bar. [d] Isosteric heat of CO_2 adsorption at zero loading.

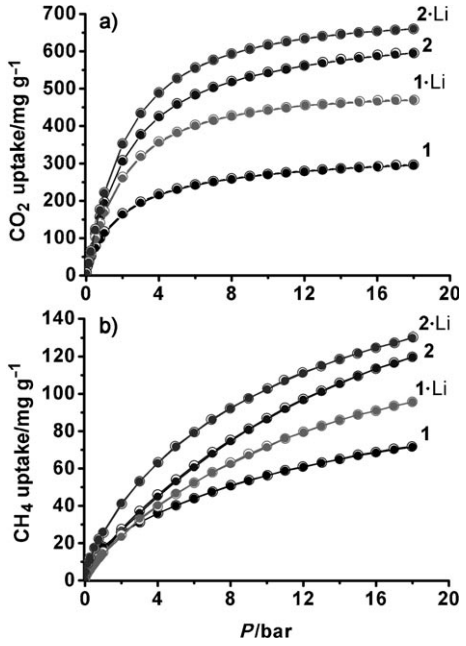

Figure 2. a) CO_2 and b) CH_4 adsorption isotherms of **1**, **1**·Li, **2**, and **2**·Li at $T = 298$ K and $P < 18$ bar. Solid and open symbols represent adsorption and desorption, respectively.

incorporation of CNTs in $[Cu_3(btc)_2]$ enhances the CO_2 and CH_4 adsorption capacities of **1** significantly.

Prior to exploring the enhancement of Li^+ ions for CO_2 adsorption, we investigated the effect of the Li content on the BET SSA of Li@$[Cu_3(btc)_2]$ (Table S1 in the Supporting Information), and observed that the BET SSA of Li@$[Cu_3(btc)_2]$ decreased rapidly as the Li/Cu ratio increased. Moreover, the PXRD patterns of the samples with Li/Cu = 16 and 73.9 are different and show new peaks at $2\theta = 32°$ (Figure S7 in the Supporting Information), thus indicating that an excess of Li^+ ions may destroy the frameworks, while the PXRD patterns of the samples with Li/Cu = 0.12 and 0.07 are consistent with that of the unmodified sample. This observation suggests that the Li content must be maintained at an appropriate low concentration in order to achieve the enhancement of gas adsorption. This conclusion is further supported by the experimental CO_2 uptake data for Li@CNT@$[Cu_3(btc)_2]$ with various Li contents (Figure S8 in the Supporting Information). Although it is very difficult to characterize the position of the Li centers owing to the inherent difficulty of obtaining single crystal of lithium-doped materials and impossibility of performing ^{7}Li NMR measurements (as Cu^{2+} ions are paramagnetic),[7d] the following explanation may be reasonable: 1) At low Li contents, the H_2O molecules in the framework Cu^{2+} sites react with the lithium naphthalenide complex to produce the thermodynamically stable lithium alkoxide species, and the two remaining hydrogen atoms combine with two naphthalenide radical anions that are present in the solvent. This hypothesis is valid as the PXRD patterns of the lithium-doped samples are unchanged compared to the unmodified $[Cu_3(btc)_2]$.[7d] 2) At high Li contents, the excessive strong nucleophilic lithium naphthalenide complex may oxidize Cu^{2+} into Cu^+ or substitute Cu^{2+} sites, which results in the collapse of the frameworks. Thus, the PXRD patterns of samples with high Li contents are different and show new peaks. This collapse of the frameworks significantly reduces the BET SSAs and subsequently inhibits the gas adsorption properties of the system.

Both CO_2 and CH_4 isotherms of **1**·Li, and **2**·Li show good reversibility without hysteresis between adsorption and desorption (Figure 2). This observation suggests that CO_2 and CH_4 are reversibly physisorbed in lithium-doped materials, similar to hydrogen storage.[7a–e] The CO_2 uptake increases from 295 mg g^{-1} (**1**) to 469 mg g^{-1} (**1**·Li) at 298 K and 18 bar, while the CH_4 uptake increases from 72 mg g^{-1} (**1**) to 96 mg g^{-1} (**1**·Li) under the same conditions. The enhancing effect of Li doping on gas adsorption is also observed for **2**. At 298 K and 18 bar, the CO_2 and CH_4 uptakes of **2**·Li reach 660 and 130 mg g^{-1}, respectively, while the uptakes are 595 and 120 mg g^{-1} in **2**, respectively, under the same conditions.

The changes in the porous properties of lithium-doped $[Cu_3(btc)_2]$ compared to unmodified $[Cu_3(btc)_2]$ were also studied by the N_2 adsorption isotherms at 77 K (Figure S6 in the Supporting Information). The isotherms exhibit completely reversible type I behavior, which is consistent with permanent microporosity. The BET SSAs of lithium-doped materials are only about half those of unmodified materials (1587 vs. 795 m^2 g^{-1} for **1** and **1**·Li, and 1458 vs. 857 m^2 g^{-1} for **2** and **2**·Li). Moreover, the pore volume of **1** drops from 0.73 cm^3 g^{-1} to 0.51 cm^3 g^{-1} after Li doping, and the pore volume of **2**·Li (0.69 cm^3 g^{-1}) is smaller than that of **2** (0.87 cm^3 g^{-1}). The Li dopant may occupy the micropores of the frameworks, thus leading to the reduction of BET SSA. However, the CO_2 and CH_4 adsorption enhancement by Li doping are clearly seen in Figure 3. The CO_2 uptake per effective SSA increases from 0.19 mg m^{-2} (**1**) to 0.59 mg m^{-2} (**1**·Li; 211 % increase), and the CH_4 uptake increases from 0.05 mg m^{-2} (**1**) to 0.12 mg m^{-2} (**1**·Li; 140 % increase), both at 298 K and 18 bar. Under the same conditions, the CO_2 uptake per effective SSA is increased from 0.41 mg m^{-2} (**2**) to 0.77 mg m^{-2} (**2**·Li; 88 % increase), and the CH_4 uptake is increased from 0.08 mg m^{-2} (**2**) to 0.15 mg m^{-2} (**2**·Li; 88 % increase). Thus, it is believed that the enhanced CO_2 and CH_4 uptakes of **1**·Li and **2**·Li are attributed to the strong affinity of the doped Li towards gas molecules, which has been confirmed by theoretical calculations.[9]

To better understand the observed enhancement, we calculated the isosteric heat of CO_2 adsorption (Q_{st}) for **1**, **1**·Li, **2**, and **2**·Li by using the Clausius–Clapeyron equation with the adsorption data (Figure S9–S12 in the Supporting Information) collected at $T = 298$, 303, 308, and 313 K and $P < 1$ bar. The Q_{st} value of **1**·Li was significantly larger than that of **1**, while the Q_{st} value of **2**·Li was slightly larger than that of **2** (Figure S13 in the Supporting Information): At zero loading, the Q_{st} values for **1** and **1**·Li are 28.0 kJ mol^{-1} and 35.7 KJ mol^{-1}, respectively, (27.5 % increase), while the Q_{st} values for **2** and **2**·Li are 34.0 and 36.8 kJ mol^{-1}, respectively (8.2 % increase). As the Li content in **2**·Li (Li/Cu = 0.001) is lower than that in **1**·Li (Li/Cu = 0.07), these results further prove that the strong affinity of Li^+ ions for CO_2 molecules is the main contribution to the gas adsorption enhancement.

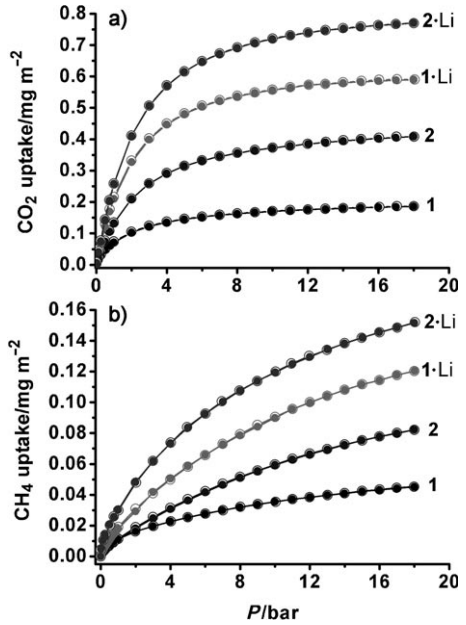

Figure 3. a) CO_2 and b) CH_4 adsorption isotherms per effective SSA of **1**, **1**·Li, **2**, and **2**·Li at $T = 298$ K and $P < 18$ bar. Solid and open symbols represent adsorption and desorption, respectively.

In summary, we have shown that incorporation of CNTs in MOFs can enhance the uptakes of CO_2 and CH_4 by MOFs. Importantly, our results show that the CO_2 and CH_4 adsorption capacities are improved by doping the CNT-modified MOFs with Li. However, excessive Li doping leads to deformation of the frameworks. In particular, the hybrid Li@CNT@$[Cu_3(btc)_2]$, which is formed by the combination of Li doping and CNT incorporation, shows CO_2 and CH_4 uptakes per effective SSA that are increased by about 305% and 200%, respectively, compared to the unmodified MOF. To achieve the enhancement, the Li content must be maintained at an appropriately low concentration. The combination of modification with CNTs and Li doping has provided a new strategy for enhancing the CO_2 and CH_4 uptakes of MOFs.

Experimental Section

CNT@$[Cu_3(btc)_2]$ was synthesized by solvothermal method. To obtain Li@CNT@$[Cu_3(btc)_2]$, a precise quantity of prepared lithium naphthalenide was transferred by syringe to a precise amount of CNT@$[Cu_3(BTC)_2]$ in THF (30 mL) in a dry flask. The mixture was stirred for 4 h and then the product was isolated by filtration and rinsed with THF, and then immersed in THF for 1 day to remove any weakly adsorbed naphthalene. Detailed experimental procedures are given in the Supporting Information.

Received: July 23, 2010
Published online: December 3, 2010

Keywords: adsorption · doping · gas storage · metal–organic frameworks · nanotubes

[1] J. D. Figueroa, T. Fout, S. Plasynski, H. Mcilvried, R. D. Srivastava, *Int. J. Greenhouse Gas Control* **2008**, *2*, 9.

[2] a) A. R. Millward, O. M. Yaghi, *J. Am. Chem. Soc.* **2005**, *127*, 17998; b) A. Demessence, D. M. D'Alessandro, M. L. Foo, J. R. Long, *J. Am. Chem. Soc.* **2009**, *131*, 8784; c) S. Q. Ma, D. F. Sun, J. M. Simmons, C. D. Collier, D. Q. Yuan, H. C. Zhou, *J. Am. Chem. Soc.* **2008**, *130*, 1012; d) S. Q. Ma, H. C. Zhou, *Chem. Commun.* **2010**, *46*, 44; e) P. L. Llewellyn, S. Bourrelly, C. Serre, A. Vimont, M. Daturi, L. Hamon, G. D. Weireld, J. S. Chang, D. Y. Hong, Y. K. Hwang, S. H. Jhung, G. Ferey, *Langmuir* **2008**, *24*, 7245; f) M. Eddaoudi, J. Kim, N. Rosi, D. Vodak, J. Wachter, M. O'Keeffe, O. M. Yaghi, *Science* **2002**, *295*, 469; g) Z. H. Xiang, J. H. Lan, D. P. Cao, X. H. Shao, W. C. Wang, D. P. Broom, *J. Phys. Chem. C* **2009**, *113*, 15106; h) P. K. Thallapally, J. Tian, M. R. Kishan, C. A. Fernandez, S. J. Dalgarno, P. B. McGrail, J. E. Warren, J. L. Atwood, *J. Am. Chem. Soc.* **2008**, *130*, 16842; i) P. K. Thallapally, C. A. Fernandez, R. K. Motkuri, S. K. Nune, J. Liu, C. H. F. Peden, *Dalton Trans.* **2010**, *39*, 1692; j) S. K. Nune, P. K. Thallapally, A. Dohnalkova, C. M. Wang, J. Liu, G. J. Exarhos, *Chem. Commun.* **2010**, *46*, 4878; k) H. Furukawa, N. Ko, Y. B. Go, N. Aratani, S. B. Choi, E. Choi, A. O. Yazaydin, R. Q. Snurr, M. O'Keeffe, J. Kim, O. M. Yaghi, *Science* **2010**, *329*, 424; l) O. K. Farha, A. O. Yazaydin, L. Eryazici, C. D. Malliakas, B. G. Hauser, M. G. Kanatzidis, S. T. Nguyen, R. Q. Snurr, J. T. Hupp, *Nat. Chem.* **2010**, *2*, 944; m) Z. H. Xiang, D. P. Cao, J. H. Lan, W. C. Wang, D. P. Broom, *Energy Environ. Sci.* **2010**, *3*, 1469; n) J. R. Li, H. C. Zhou, *Nat. Chem.* **2010**, *2*, 893.

[3] a) H. Furukawa, O. M. Yaghi, *J. Am. Chem. Soc.* **2009**, *131*, 8875; b) T. Ben, H. Ren, S. Q. Ma, D. P. Cao, J. H. Lan, X. F. Jing, W. C. Wang, J. Xu, F. Deng, J. M. Simmons, S. L. Qiu, G. S. Zhu, *Angew. Chem.* **2009**, *121*, 9621; *Angew. Chem. Int. Ed.* **2009**, *48*, 9457; c) H. M. El-Kaderi, J. R. Hunt, J. L. Mendoza-Cortes, A. P. Cote, R. E. Taylor, M. O'Keeffe, O. M. Yaghi, *Science* **2007**, *316*, 268; d) J. H. Lan, D. P. Cao, W. C. Wang, T. Ben, G. S. Zhu, *J. Phys. Chem. Lett.* **2010**, *1*, 978.

[4] a) S. J. Yang, J. Y. Choi, H. K. Chae, J. H. Cho, K. S. Nahm, C. R. Park, *Chem. Mater.* **2009**, *21*, 1893; b) A. W. Thornton, K. M. Nairn, J. M. Hill, A. J. Hill, M. R. Hill, *J. Am. Chem. Soc.* **2009**, *131*, 10662; c) Z. Q. Wang, S. M. Cohen, *Chem. Soc. Rev.* **2009**, *38*, 1315.

[5] a) J. T. Han, S. Y. Kim, J. S. Woo, G.-W. Lee, *Adv. Mater.* **2008**, *20*, 3724; b) S. Berson, R. De Bettignies, S. Bailly, S. Guillerez, B. Jousselme, *Adv. Funct. Mater.* **2007**, *17*, 3363.

[6] M. Shoaee, M. W. Anderson, M. P. Attfield, *Angew. Chem.* **2008**, *120*, 8653; *Angew. Chem. Int. Ed.* **2008**, *47*, 8525.

[7] a) S. H. Yang, X. Lin, A. J. Blake, G. S. Walker, P. Hubberstey, N. R. Champness, M. Schroder, *Nat. Chem.* **2009**, *1*, 487; b) K. L. Mulfort, J. T. Hupp, *J. Am. Chem. Soc.* **2007**, *129*, 9604; c) K. L. Mulfort, T. M. Wilson, M. R. Wasielewski, J. T. Hupp, *Langmuir* **2009**, *25*, 503; d) D. Himsl, D. Wallacher, M. Hartmann, *Angew. Chem.* **2009**, *121*, 4710; *Angew. Chem. Int. Ed.* **2009**, *48*, 4639; e) A. Li, R. F. Lu, Y. Wang, X. Wang, K. L. Han, W. Q. Deng, *Angew. Chem.* **2010**, *122*, 3402; *Angew. Chem. Int. Ed.* **2010**, *49*, 3330; f) D. P. Cao, J. H. Lan, W. C. Wang, B. Smit, *Angew. Chem.* **2009**, *121*, 4824; *Angew. Chem. Int. Ed.* **2009**, *48*, 4730; g) S. S. Han, W. A. Goddard III, *J. Am. Chem. Soc.* **2007**, *129*, 8422; h) S. S. Han, W. A. Goddard III, *J. Phys. Chem. C* **2008**, *112*, 13431.

[8] J. H. Lan, D. P. Cao, W. C. Wang, *Langmuir* **2009**, *26*, 220.

[9] J. H. Lan, D. P. Cao, W. C. Wang, B. Smit, *ACS Nano* **2010**, *4*, 4225.

[10] a) S. S.-Y. Chui, S. M. F. Lo, J. P. H. Charmant, A. G. Orpen, I. D. Williams, *Science* **1999**, *283*, 1148; b) Z. H. Xiang, D. P. Cao, X. H. Shao, W. C. Wang, J. W. Zhang, W. Z. Wu, *Chem. Eng. Sci.* **2010**, *65*, 3140.

[11] C. Prestipino, L. Regli, J. G. Vitillo, F. Bonino, A. Damin, C. Lambert, A. Zecchina, P. L. Solari, K. O. Kongshaug, S. Bordiga, *Chem. Mater.* **2006**, *18*, 1337.

